Journal of the Meteorological Society of Japan, Vol. 92A, 195−203, 2014
DOI:10.2151/jmsj.2014-A13

Column Water Vapor Retrievals from Sky Radiometer (POM-02) 940 nm Data

Akihiro UCHIYAMA, Akihiro YAMAZAKI, and Rei KUDO

Meteorological Research Institute, Japan Meteorological Agency, Tsukuba, Japan

(Manuscript received 14 November 2013, in final form 4 June 2014)

Abstract

Sky radiometer data are used to retrieve aerosol optical properties and to estimate the effect of aerosols on solar irradiance at the Earth's surface. The Prede POM-02 is equipped with a 940-nm channel corresponding to a primary water vapor absorption band in the near infrared region, but 940-nm data have been underutilized. Atmospheric water vapor is an important factor in determining the surface radiation budget. To retrieve the columnar precipitable water vapor amount from sun-sky radiometers, the 940-nm channel was calibrated using the Langley method, which accounts for gas absorption. The relation between column water vapor and atmospheric transmittance at 940 nm was determined using simulation data, and the results were used to retrieve column water vapor. This method was applied to data collected at Tsukuba, Japan, in 2011 and compared with global positioning system receiver (GPS), microwave radiometer, and radiosonde water vapor retrievals. The highest correlations were found between GPS and radiosonde observations. A comparison of POM-02 and GPS results showed a bias error of 0.09 g cm^{-2}; the root mean square error was 0.179 g cm^{-2}; and r = 0.996. The transmittance of the 940-nm channel was theoretically determined in this study. Therefore, the accuracy of column water vapor retrieval depends on the accuracy of transmittance calculation model.

Keywords column water vapor; precipitable water vapor; sky radiometer

1. Introduction

A sky radiometer (POM-01 and POM-02, Prede Co., Ltd.) measures direct solar irradiance and diffuse sky radiances in the visible to near-infrared spectral range (see Table 1). Data in the visible to near-infrared spectrum, wavelengths less than 1050 nm, are used to retrieve aerosol optical properties and estimate the effect of aerosols on the Earth's radiation budget. POM-02 has additional channels in the near-infrared region, at 1627 nm and 2200 nm. Using these channels, cloud physical properties can be retrieved (Kikuchi et al. 2006).

POM-02 also has a 940-nm channel that can be used to estimate column water vapor (precipitable water vapor, PWV), inferred from measurements of direct solar irradiance attenuation in clear sky conditions. Water vapor is an important constituent of the Earth's climate system and has a large effect on the Earth's radiation budget. Furthermore, the use of 1627-nm and 2200-nm channels requires knowledge of the water vapor amount because water vapor absorbs electromagnetic energy in these wavelength regions as well.

A sky radiometer is the primary instrument within SKY radiometer NETwork (SKYNET, http://atmos.cr.chiba-u.ac.jp/), which is an observation network designed to understand aerosol-cloud-radiation interaction in the atmosphere (Takamura et al. 2004). In spite of the importance of water vapor, the 940-nm channel has not been extensively used, and a better understanding of the utility of this channel for PWV retrievals would be useful.

Methods to retrieve PWV from the attenuation of direct solar irradiance were first reported by Fowle

Corresponding author: Akihiro Uchiyama, Meteorological Research Institute, Japan Meteorological Agency, 1-1 Naganine, Tsukuba, Ibaraki 305-0052, Japan
E-mail: uchiyama@mri-jma.go.jp

Table 1. Comparison of PWV computations.

Wavelength (nm)	POM-01	POM-02	POM-02 (MRI)	FWHM (nm)	Detector
315(±0.6)	○	○	–	3(±0.6)	Si photodiode
340(±0.6)	○	○	○	3(±0.6)	
380(±0.6)	○	○	○	3(±0.6)	
400(±2.0)	○	○	○	10(±2.0)	
500(±2.0)	○	○	○	10(±2.0)	
675(±2.0)	○	○	○	10(±2.0)	
870(±2.0)	○	○	○	10(±2.0)	
940(±2.0)	○	○	○	10(±2.0)	
1020(±2.0)	○	○	○	10(±2.0)	
1225(±2.0)	–	–	○	10(±2.0)	InGaAs photodiode
1627(±2.0)	–	○	○	20(±4.0)	
2200(±2.0)	–	○	○	20(±4.0)	

FWHM: full width at half maximum

(1912, 1915). In recent years, many papers have been published describing PWV retrievals by means of ground-based sun photometry (Reagan et al. 1987a, 1987b, 1995; Bruegge et al. 1992; Thome et al. 1992, 1994; Michalsky et al. 1995, 2001; Schmid et al. 1996, 2001; Shiobara et al. 1996; Halthore et al. 1997; Cachorro et al. 1998; Plana-Fattori et al. 1998, 2004; Ingold et al. 2000; Kiedron et al. 2001, 2003). Methods for retrieving PWV using Aerosol Robotic NETwork (AERONET) sun-sky radiometers operating at 940 nm were reported by Holben et al. (1998). More recently, Campanelli et al. (2013) reported the Surface Humidity Method (SHM), which uses columnar water vapor that is estimated from standard meteorological measurements (temperature, pressure, and relative humidity).

The purpose of this study was to develop a new method to retrieve PWV from POM-01 and POM-02 940-nm data.

2. Methods

2.1 Calibration of the 940-nm channel

To retrieve PWV from measurements of direct solar irradiance, the sky radiometer must be calibrated. The sensor output can be written as

$$V = C\frac{1}{R^2}\frac{1}{\Delta\lambda}\int_{\Delta\lambda}\varphi(\lambda)T_{gas}(\lambda)T_{aer}(\lambda)T_{mol}(\lambda)F_0(\lambda)d\lambda, \quad (1)$$

where V is sensor output voltage, C is a proportionality constant, $\varphi(\lambda)$ is the filter response function, $F_0(\lambda)$ is the solar irradiance outside of the terrestrial atmosphere at wavelength λ, $T_{gas}(\lambda)$ is the transmittance of absorbing gases, $T_{aer}(\lambda)$ is the transmittance of aerosols, $T_{mol}(\lambda)$ is the transmittance due to molecular scattering, and R is the distance between the Earth and the sun in astronomical units.

Since the channel width, $\Delta\lambda$, is narrow, full width at half maximum is 10 nm, and the changes in the transmittance of aerosols and molecular scattering across the channel width are small, the transmittances $T_{aer}(\lambda)$ and $T_{mol}(\lambda)$ can be approximated by $T_{aer}(\lambda) \cong T_{aer}(\lambda = 940\ nm)$ and, $T_{mol}(\lambda) \cong T_{mol}(\lambda = 940\ \mathrm{nm})$ respectively. Furthermore, $F_0(\lambda)$ is approximated by $F_0(\lambda) = F_0(\lambda = 940\ nm)$. Using these approximations, Eq. (1) can be rewritten as follows:

$$V \cong V_0\frac{1}{R^2}T_{aer}(\lambda = 940\ \mathrm{nm})T_{mol}(\lambda = 940\ \mathrm{nm})\overline{T}_{gas}, \quad (2)$$

where

$$V_0 \equiv CF_0(\lambda = 940\ \mathrm{nm}), \quad (3)$$

$$\overline{T}_{gas} = \frac{1}{\Delta\lambda}\int_{\Delta\lambda}\varphi(\lambda)T_{gas}(\lambda)d\lambda, \quad (4)$$

V_0 is a calibration constant (instrument constant), and $\overline{T}_{gas}$ is the band average transmittance.

Since at 940 nm water vapor is the dominant absorbing constituent, only water vapor absorption is considered: $\overline{T}_{gas} = \overline{T}_{\mathrm{H2O}}$.

Using $T_{aer}(\lambda = 940\ \mathrm{nm})T_{mol}(\lambda = 940\ \mathrm{nm}) = \exp(-m(\tau_{aer} + \tau_R))$, Eq. (2) can be rewritten as follows:

$$V = \frac{V_0}{R^2}\overline{T}_{\mathrm{H2O}}\exp(-m(\tau_{aer} + \tau_R)), \quad (5)$$

where m is airmass, τ_{aer} is the aerosol optical thickness at 940 nm, and τ_R is the optical thickness due to molecular scattering (Rayleigh scattering) at 940 nm.

Rearranging Eq. (5) and applying a logarithmic transform yields

$$\ln(VR^2/\overline{T}_{\mathrm{H2O}}) = \ln V_0 - m(\tau_{aer} + \tau_R). \quad (6)$$

Given the vertical profile of atmospheric temperature and humidity and by estimating $\overline{T}_{\mathrm{H2O}}$ using radiative transfer code to calculate atmospheric transmittance, Eq. (6) may be used to determine V_0 using the Langley method, where the x-axis is m and the y-axis is $\ln(VR^2/\overline{T}_{\mathrm{H2O}})$. Data for the Langley method were recorded at the NOAA Mauna Loa Observatory; 3397 m asl, 19.5362°N, 155.5763°W. The measurements of POM-02 were made every 1 min from sunrise to sunset. PWV derived from GPS installed at the NOAA Mauna Loa Observatory could be obtained every 30 min. The radiosonde observations at Hilo, Hawaii, were made twice a day at 00:00 and 12:00 UTC. Atmospheric transmittance was computed every 1 min using interpolated radiosonde observation of vertical temperature and water vapor. The column water vapor was changed to the value derived from GPS, which was also interpolated to the POM-02 observation time.

In the example Langley plot (Fig. 1), the regression line was determined using the data between airmass $m = 2$ and $m = 6$. On the stable condition, the accurate regression line could be represented as in the example.

The atmospheric transmittance is weighted by the response function of the interference filter, which has a half value bandwidth of about 10 nm. Atmospheric transmittance was computed using the correlated-k distribution method (Lacis et al. 1979; Lacis and Oinas 1991). The correlated-k distribution data was created with the 10-nm interval. Therefore, the response function was approximated using a stepwise function with a 10-nm bandwidth. The height of the stepwise function for each band interval was determined as the area of the original response function for every band interval. Atmospheric transmittance computations also account for the curvature of the Earth and the refraction of the solar path. The database of the correlated-k distribution was calculated on the basis of the 1996 version of HITRAN data (Rothman et al. 1998) using computer code reported by Uchiyama (1992). HITRAN line intensities at 940 nm were revised in 2000 and 2004 (Giver et al. 2000; Belmiloud et al. 2000; Schermaul et al. 2001a, b; Rothman et al. 2005). Therefore, there is a possibility that the atmospheric transmittance computation in this study has an error. Alexandrov et al. (2009) compared slant path optical depth at 940 nm derived from observations using a Multi-filter, Rotating Shadowband Radiometer (MFRSR), microwave radiometer (MWR), and models based on HITRAN 1996, 2000, and 2004 data. Their results (shown in their Fig. 2) indicate that the 1996 HITRAN data are not significantly different, and therefore, the use of HITRAN 1996 does not cause a serious error.

2.2 *Relation between PWV and water vapor transmittance*

R and m in Eq. (5) were calculated using the time and position of observations. The molecular scattering optical thickness (τ_R) was calculated from the surface atmospheric pressure. The aerosol optical thickness (τ_{aer}) at 940 nm was estimated by interpolation from observations made at 875 nm and 1020 nm. If V_0 is known, the transmittance of water vapor $\overline{T}_{\mathrm{H2O}}$ in Eq. (5) can be obtained from the measurement of direct solar irradiance. Therefore, given the relation between $\overline{T}_{\mathrm{H2O}}$ and precipitable water vapor, PWV can be determined.

The transmittance of water vapor $\overline{T}_{\mathrm{H2O}}$ is typically approximated with an empirical equation (Moskalenko 1969; Pitts et al. 1974, 1977; Koepke and Quenzel 1978; Bruegge et al. 1992),

$$\overline{T}_{\mathrm{H2O}} = \exp(-a(m \cdot \mathrm{PWV})^b), \quad (7)$$

where the coefficients a and b are adjustable parameters. Some studies have used a more restrictive approximation, where $b = 0.5$ (Gates and Harrop 1963; Reagan et al. 1987a, b).

In this study, the relation between $\overline{T}_{\mathrm{H2O}}$ and PWV was determined using simulation data. Given the model atmosphere, transmittances were calculated under 8 different conditions to simulate a large range of path length (airmass = 15.2–1.1): transmittances were calculated at 6:40, 7:00, 7:30, 8:00, 8:30, 9:00, 10:00, and 11:00 on vernal equinox at 19.539°N and 155.578°W, which are the co-ordinates of the Mauna Loa observatory. Furthermore, 10 different model atmospheres were used: five atmospheric models (tropical, mid-latitude summer and winter, and sub-arctic summer and winter) reported by McClatchey et al. (1972), four modifications of the McClatchey et al. models, excluding the tropical atmosphere, using one-tenth of the original PWV value, and the U.S. 1962 standard atmosphere.

Then, Eq. (7) can be rewritten as follows:

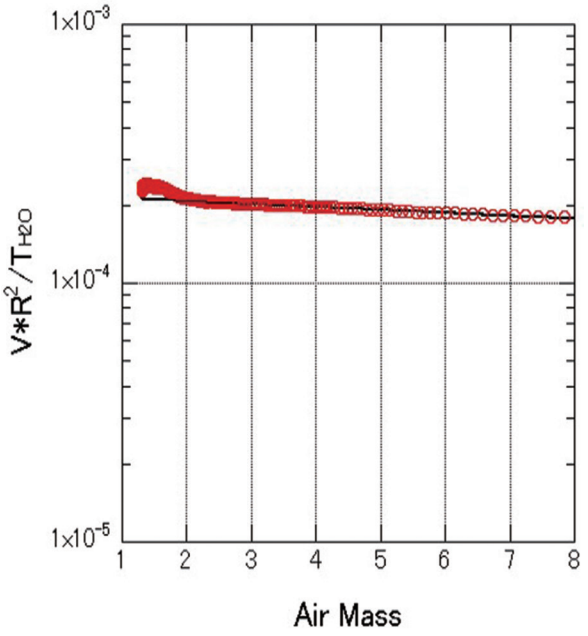

Fig. 1. An example Langley plot for the POM-02 940-nm-water-vapor channel. The data were obtained on November 23, 2009 at the NOAA Mauna Loa Observatory. The regression line was computed using data between airmasses 2 and 6.

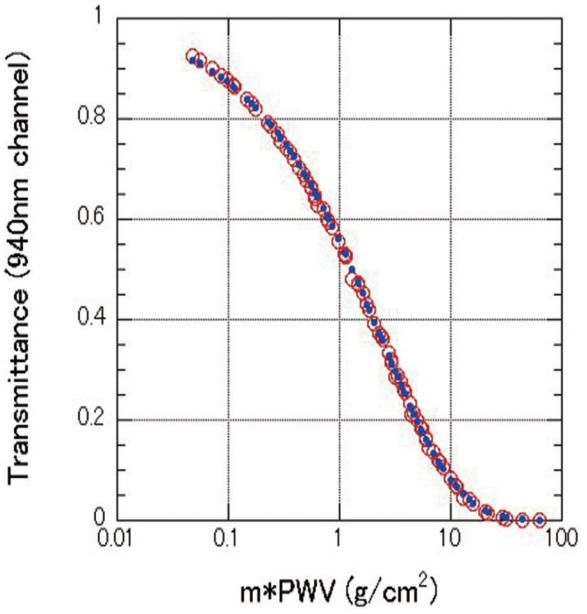

Fig. 2. Relation between perceptible water vapor (PWV) and channel average transmittance. Open circles are theoretical values and close circles are values calculated with the empirical formula.

$$\ln \overline{T}_{\mathrm{H2O}} = -a(m \cdot \mathrm{PWV})^b. \quad (8)$$

Using the data set relating $\overline{T}_{\mathrm{H2O}}$ and PWV, we determined the coefficients a and b using the following procedure. Given values for b, a was determined by the method of least squares, and the root mean square error (RMSE) was calculated. The method of least squares was applied between $\ln \overline{T}_{\mathrm{H2O}}$ and $(m \cdot \mathrm{PWV})^b$. The coefficient b was systematically adjusted between 0.5 and 1.0 until a value was identified that minimized the RMSE to three significant figures; the step of variability of b is 0.001.

The coefficients a and b depend on the vertical structure of atmospheric temperature and humidity. Therefore, it is difficult to choose suitable values that can be applied to all atmospheric conditions. In reality, the range of variability of transmittance for an atmospheric profile is limited. Atmospheric transmittance was computed for a broad range of atmospheric conditions, and best fit values of the ensemble conditions were chosen for a and b (Fig. 2).

The relation between $\overline{T}_{\mathrm{H2O}}$ and PWV can be determined using $\overline{T}_{\mathrm{H2O}}$ measured by POM-02 and PWV calculated from radiosonde data. In our observation site, radiosonde observation at 00.00 UTC (09.00 LT) can be used. The range of airmass is from 1.2 in summer to 3 in winter at 09 LT. Furthermore, the range of PWV is from 0.5 g cm^{-2} in winter to 5 g cm^{-2} in summer. Therefore, the range of $m \cdot \mathrm{PWV}$ is from 1.5 to 6, and the range of transmittance for fitting an equation is limited.

2.3 *Field measurements*

Using Eq. (6), PWV was determined from the measurements of direct solar irradiance attenuation of POM-02 940-nm channel in clear sky conditions. Two POM-02 instruments were used in this comparison study. One (S.N. PS1207831) was calibrated using data recorded at the NOAA Mauna Loa Observatory and served as a reference, and the other (S.N. PS1202091) was calibrated by comparing the two sensor outputs of direct solar irradiance. Thus, the calibration constant for the second instrument was transferred from the reference instrument.

Moreover, PWV was measured by other instruments, GPS, and MWR data. PWV was also calculated using radiosonde data. MWR (TP/WVP-3000, Radiometric Corporation) was collocated with POM-02.The GPS station (Ami, Station No. 0584) is located about 8 km ESE of the observation site.

Table 2. Results of the comparisons.

Radiosonde vs. MWR PWV, Radiosonde vs. GPS PWV

	Bias	Bias (median)	RMSE	r	C_1	C_2
Radiosonde vs. MWR	0.148	0.115	0.219	0.997	1.048	0.030
Radiosonde vs. GPS	–0.042	–0.048	0.124	0.9996	0.9995	–0.041

GPS vs. POM-02 PWV

	Bias	Bias (median)	RMSE	r	C_1	C_2
GPS vs. POM-02 (PS1207831)	0.090	0.114	0.179	0.996	0.957	0.169
GPS vs. POM-02 (PS1202091)	0.033	0.084	0.198	0.996	0.924	0.199

Bias: g cm^{-2}; RMSE: root mean square error, g cm^{-2}; r: correlation coefficient; C_1 and C_2: coefficients of regression line ($PWV_a = C_1 \times PWV_b + C_2$).

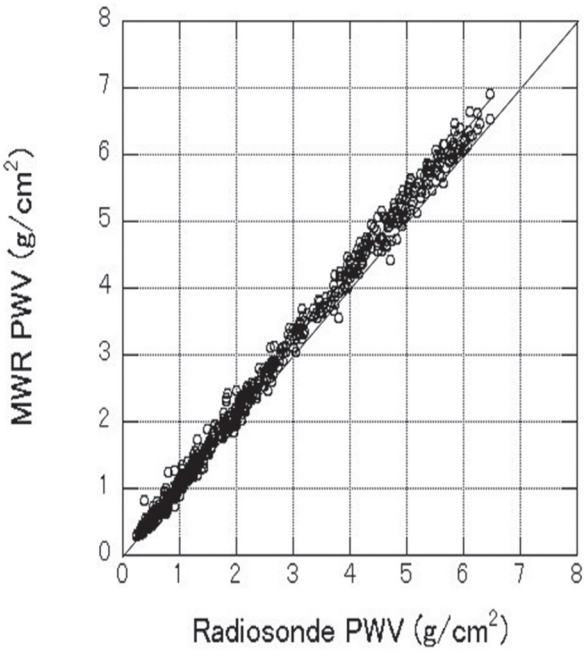

Fig. 3. Comparison between radiosonde and GPS derived PWV.

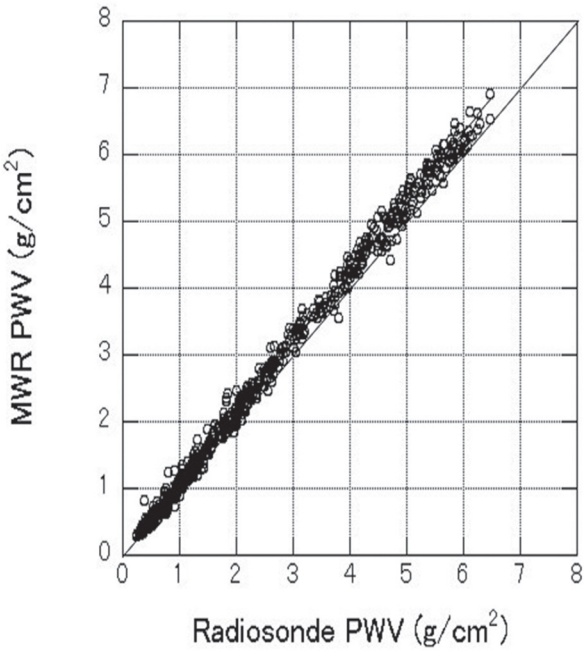

Fig. 4. Comparison between radiosonde and MWR derived PWV.

The radiosonde's site (Taneno, Station No. 47646) is located adjacent to POM-02 and the MWR site.

Data were collected from January through December 2011. However, measurement operations were stopped on some days in February, March, and December and on all days in August and November. Furthermore, PWV retrieval from POM-02 data during cloudy conditions is corrupted, and the retrieval cannot be performed at night.

3. Results

PWV determinations from radiosonde, GPS, MWR, and POM-02 were compared using least squares regression analyses (Table 2). Radiosonde and GPS-derived PWV were highly correlated (Fig. 3). The bias (GPS-Radiosonde) error was −0.042

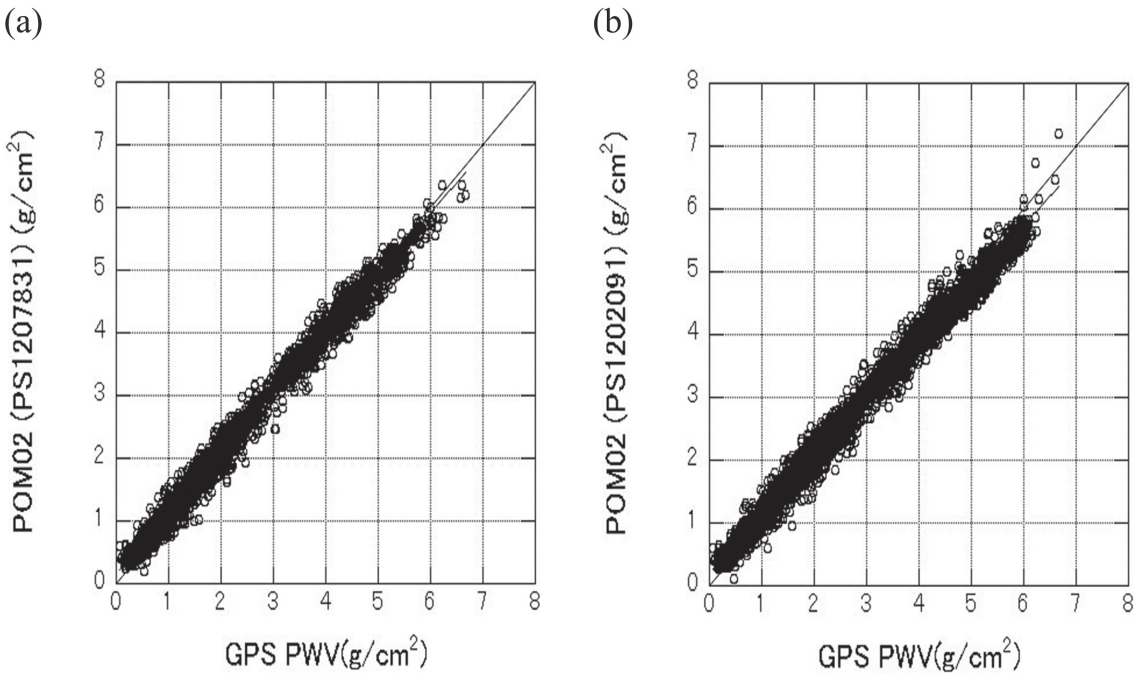

Fig. 5. Comparison between GPS and POM-02 derived PWV. (a) POM-02 reference instrument (S.N. PS1207831) was calibrated using data recorded at the NOAA Mauna Loa Observatory. (b) POM-02 (S.N. PS1202091) was calibrated to the reference POM-02 instrument (S.N. PS1207831).

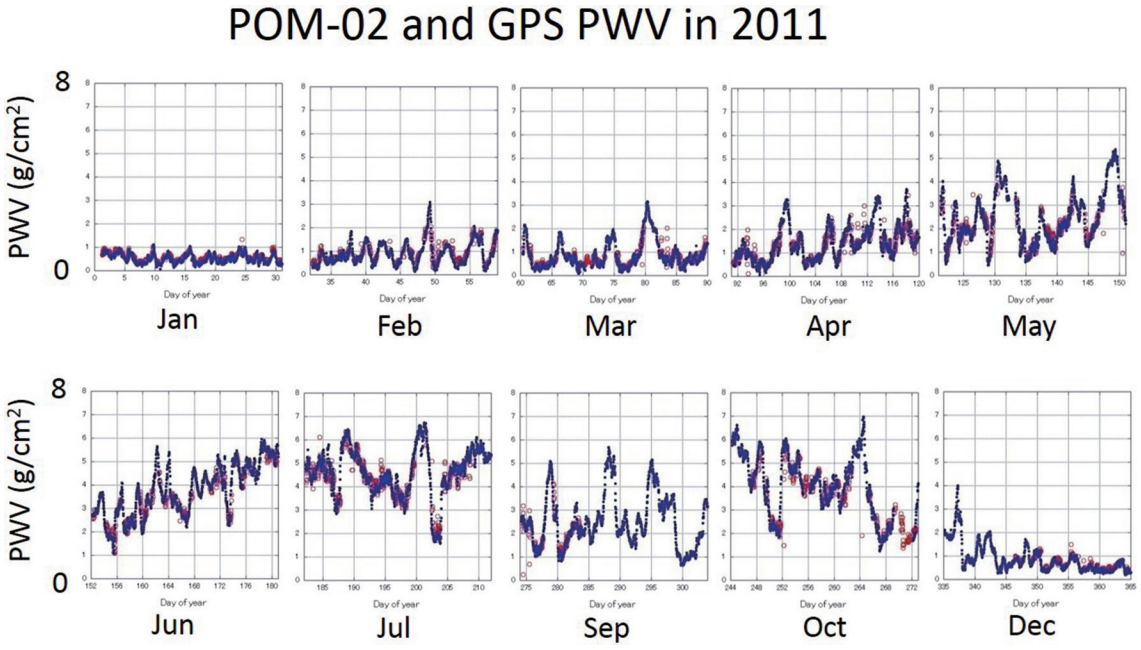

Fig. 6. Time series of 30 min averaged PWV derived from POM-02 (red open circles) and GPS (blue solid circles) data recorded in 2011 at Tsukuba, Japan.

g cm^{-2}, RMSE was 0.124 g cm^{-2}, and r = 0.9996. Linear regression coefficients [(GPS PWV) = C_1 × (radiosonde PWV) + C_2] are C_1 = 0.9995 and C_2 = −0.041. Radiosonde and MWR-derived PWV values were also highly correlated, and the correlation was only slightly weaker than that with GPS values (Fig. 4). The bias (MWR-Radiosonde) error was 0.148 g cm^{-2}, RMSE was 0.219 g cm^{-2}, and r = 0.997. The linear regression coefficients [(MWR PWV) = C_1 × (radiosonde PWV) + C_2] are C_1 = 1.048 and C_2 = 0.030. The MWR PWV is larger than the corresponding radiosonde PWV in regions of high water vapor content.

PWV determined from POM-02 observations (reference instrument, S.N. PS1207831) were highly correlated with GPS determinations (Fig. 5a). The bias (POM-02–GPS) error was 0.090 g cm^{-2}, RMSE was 0.179 g cm^{-2}, and r = 0.996. The coefficients of linear regression [(POM-02 PWV) = C_1 × (GPS PWV) + C_2] between them are C_1 = 0.957 and C_2 = 0.169. In regions of elevated water vapor content, POM-02 PWV is slightly smaller than the GPS values. PWV determined from the second POM-02 instrument (S.N. PS1202091) was also highly correlated with GPS values (Fig. 5b). The bias (POM-02–GPS) error was 0.033 g cm^{-2}, RMSE was 0.198 g cm^{-2}, and r = 0.996. The coefficients of linear regression [(POM-02 PWV) = C_1 × (GPS PWV) + C_2] are C_1 = 0.924 and C_2 = 0.199. There are some differences between values derived from the two POM-02 instruments. In this comparison, a and b were held constant. The coefficients depend on the filter response function. The differences, apparent in Fig. 5, reflect the different filter response functions. These differences show that it is necessary to determine the coefficients a and b instrument by instrument.

MWR PWV values tended to be larger than POM-02 values (data not shown) in the regions of elevated water vapor content, as was suggested by the comparison of radiosonde and MWR retrievals.

Time series of PWV, computed as 30 min averages, from POM-02 and GPS data recorded at Tsukuba, Japan, in 2011, are highly correlated (Fig. 6). There are no large or systematic trends in the differences between the two retrievals.

4. Summary and conclusions

A method to retrieve precipitable atmospheric water vapor from POM-02 940-nm data was developed and compared with other estimations of PWV from radiosonde, GPS, and MWR. POM-02 data were calibrated against data recorded at the NOAA Mauna Loa Observatory by the Langley method, taking water vapor absorption into account. A relation between PWV and water vapor transmittance ($\overline{T}_{\mathrm{H2O}}$) was derived on the basis of the simulated data. Given atmospheric models and POM-02 filter response functions, atmospheric transmittance at 940 nm was calculated for various airmasses, and coefficients of empirical formula were determined.

Comparisons of PWV derived from POM-02, GPS, radiosonde, and MWR observations using data recorded in 2011 at Tsukuba, Japan, revealed correlations between GPS and radiosonde PWV determinations: the bias error was −0.042 g cm^{-2}, RMSE was 0.124 g cm^{-2}, and r = 0.9996. The comparison between GPS and POM-02 PWV resulted in a bias error of 0.090 g cm^{-2}, RMSE = 0.179 g cm^{-2}, and r = 0.996.

Acknowledgment

The authors are extremely grateful to Dr. Y. Shoji for providing the GPS precipitable water vapor data. We also express our appreciation to two anonymous reviewers for their useful comments. This research was partially supported by the Environment Research and Technology Development Fund (2A-1102) of the Ministry of the Environment, Japan.

References

Alexandrov, M. D., B. Schmid, D. D. Turner, B. Cairns, V. Oinas, A. A. Lacis, S. I. Gutman, E. R. Westwater, A. Smirnov, and J. Eilers, 2009: Columnar water vapor retrievals from multifilter rotating shadowband radiometer data. *J. Geophys. Res.*, **114**, D02306, doi:10.1029/2008JD010543.

Belmiloud, D., R. Schermaul, K. M. Smith, N. F. Zobov, J. W. Brault, R. C. M. Learner, D. A. Newnham, and J. Tennyson, 2000: New studies of the visible and near-infrared absorption by water vapour and some problems with the HITRAN database. *Geophys. Res. Lett*., **27**, 3703– 3706.

Bruegge, C. J., J. E. Conel, R. O. Green, J. S. Margolis, R. G. Holm, and G. Toon, 1992: Water vapor column abundance retrievals during FIFE. *J. Geophys. Res.*, **97**, 18759–18768.

Cachorro, V. E., P. Utrillas, R. Vergaz, P. Duran, A. M. de Frutos, and J. A. Martinez-Lozano, 1998: Determination of the atmospheric-water-vapor content in the 940-nm absorption band by use of moderate spectral-resolution measurements of direct solar irradiance. *Appl. Opt*., **37**, 4678–4689.

Campanelli, M., T. Nakajima, P. Khatri, T. Takamura, A. Uchiyama, V. Estelles, G. L. Liberti, and V. Malvestuto, 2013: Retrieval of characteristic parameters for

water vapour transmittance in the development of ground based sun-sky radiometric measurements of columnar water vapour. *Atmos. Meas. Tech.* **7**, 1075–1087.

Fowle, F. E., 1912: The spectroscopic determination of aqueous vapor. *Astrophys. J.*, **35**, 149–162.

Fowle, F. E. ,1915: The transparency of aqueous vapor. *Astrophys. J.*, **42**, 394–411.

Gates, D. M., and W. J. Harrop, 1963: Infrared transmission of the atmosphere to solar radiation. *Appl. Opt*., **2**, 887–898.

Giver, L. P., C. Chackerian Jr., and P. Varanasi, 2000: Visible and near-infrared $H_2{}^{16}O$ line intensity corrections for HITRAN-96. *J. Quant. Spectrosc. Radiat. Transfer*, **66**, 101–105.

Halthore, R. N., T. F. Eck, B. N. Holben, and B. L. Markham, 1997: Sun photometric measurements of atmospheric water vapor column abundance in the 940-nm band. *J. Geophys. Res*., **102**, 4343–4352.

Holben, B. N., T. F. Eck, I. Slutsker, D. Tanré, J. P. Buis, A. Setzer, E. Vermote, J. A. Reagan, Y. J. Kaufman, T. Nakajima, F. Lavenu, I. Jankowiak, and A. Smirnov, 1998: AERONET-A federated instrument network and data archive for aerosol characterization. *Remote Sens. Environ.*, **66**, 1–16.

Ingold, T., B. Schmid, C. Matzler, P. Demoulin, and N. Kampfer, 2000: Modeled and empirical approaches for retrieving columnar water vapor from solar transmittance measurements in the 0.72, 0.82, and 0.94 mm absorption bands. *J. Geophys. Res.*, **105**, 24327–24343.

Kiedron, P., J. Michalsky, B. Schmid, D. Slater, J. Berndt, L. Harrison, P. Racette, E. Westwater, and Y. Han, 2001: A robust retrieval of water vapor column in dry Arctic conditions using the rotating shadowband spectroradiometer. *J. Geophys. Res*., **106**, 24007–24016.

Kiedron, P., J. Berndt, J. Michalsky, and L. Harrison, 2003: Column water vapor from diffuse irradiance. *Geophys. Res. Lett.*, **30**, 1565, doi:10.1029/2003GL016874.

Kikuchi, N., T. Nakajima, H. Kumagai, H. Kuroiwa, A. Kamei, R. Nakamura, and T. Y. Nakajima, 2006: Cloud optical thickness and effective particle radius derived from transmitted solar radiation measurements: Comparison with cloud radar observations. *J. Geophys. Res.*, **111**, D07205, doi:10.1029/2005JD006363.

Koepke, P., and H. Quenzel, 1978: Water vapor: spectral transmission at wavelengths between 0.7 mm and 1 mm. *Appl. Opt*., **17**, 2114–2118.

Lacis, A. A., and V. Oinas, 1991: A description of the correlated k distribution method for modeling nongray gaseous absorption, thermal emission, and multiple scattering in vertically inhomogeneous atmospheres. *J. Geophys. Res.*, **96**, 9027–9063.

Lacis, A. A., W. C. Wang, and J. E. Hansen, 1979: Correlated k-distribution method for radiative transfer in climate models: Application to effect of cirrus clouds on climate. *NASA Conf. Publ.,* **2076**, 309–314.

Michalsky, J. J., J. C. Liljegren, and L. C. Harrison, 1995: A comparison of sun photometer derivations of total column water vapor and ozone to standard measures of same at the Southern Great Plains atmospheric radiation measurement site. *J. Geophys. Res*., **100**, 25995–26003.

Michalsky, J. J., Q. Min, P. W. Kiedron, D. W. Slater, and J. C. Barnard, 2001: A differential technique to retrieve column water vapor using sun radiometry. *J. Geophys. Res.*, **106**, 17433–17442.

McClatchey, R. A., R. W. Fenn, J. E. A. Selby, F. E. Volz, and J. S. Garing, 1972: *Optical properties of the atmosphere, 3rd edition*. Air Force Cambridge Reserch Labs Hanscom Air Force Base, No. AFCRL-72-0497, MA.

Moskalenko, N. I., 1969: The spectral transmission function in the bands of water vapor, O_3, N_2O and N_2 atmospheric components. *Izv. Akad. Sci. USSR Atmos. Oceanic Phys*., **5**, 1178–1178.

Pitts, D. E., W. McAllum, and A. E. Dillinger, 1974: *Measurement of atmospheric precipitable water using a solar radiometer*. NASA Tech. Memo, X-58129, NASA L. B. Johnson Space Cent., Houston, TEX, USA.

Pitts, D. E., W. E. McAllum, M. Heidt, K. Jeske, J. T. Lee, D. DeMonbrun, A. Morgan, and J. Potter, 1977: Temporal variations in atmospheric water vapor and aerosol optical depth determined by remote sensing. *J. Appl. Meteor.*, **16**, 1312–1321.

Plana-Fattori, A., M. Legrand, D. Tanre, C. Devaux, A. Vermeulen, and P. Dubuisson, 1998: Estimating the atmospheric water vapor content from sun photometer measurements. *J. Appl. Meteor.*, **37**, 790– 804.

Plana-Fattori, A., P. Dubuisson, B. A. Fomin, and M. de P. Correa, 2004: Estimating the atmospheric water vapor content from multi-filter rotating shadow-band radiometry at Sao Paulo, Brazil. *Atmos. Res.*, **71**, 171–192.

Reagan, J. A., K. Thome, B. Herman, and R. Gall, 1987a: Water vapor measurements in the 0.94 micron absorption band-Calibration, measurements and data applications. *Proceeding of Int. Geoscience and Remote Sensing '87 Symposium,* 63–67.

Reagan, J. A., P. A. Pilewskie, B. M. Herman, and A. Ben-David, 1987b: Extrapolation of earth-based solar irradiance measurements to exoatmospheric levels for broad-band and selected absorption-band observations. *IEEE Trans. Geosci. Remote Sens.*, **25**, 647–653.

Reagan, J., K. Thome, B. Herman, R. Stone, J. DeLuisi, and J. Snider, 1995: A comparison of columnar water vapor retrievals obtained with near-IR solar radiometer and microwave radiometer measurements. *J.*

Appl. Meteor., **34**, 1384–1391.

Rothman, L. S., C. P. Rinsland, A. Goldman, S. T. Massie, D. P. Edwards, J. M. Flaud, A. Perrin, C. Camy-Peyret, V. Dana, J. Y. Mandin, J. Schroeder, A. McCann, R. R. Gamache, R. B. Wattson, K. Yoshino, K. V. Chance, K. W. Jucks, L. R. Brown, V. Nemtchinov, and P. Varanasi, 1998: The HITRAN molecular spectroscopic database and HAWKS (HITRAN atmospheric workstation): 1996 edition. *J. Quant. Spectrosc. Radiat. Transfer*, **60**, 665–710.

Rothman, L. S., D. Jacquemart, A. Barbe, D. Chris Benner, M. Birk, L. R. Brown, M. R. Carleer, C. Chackerian Jr., K. Chance, L. H. Coudert, V. Dana, V. M. Devi, J.-M. Flaud, R. R. Gamache, A. Goldman, J.-M. Hartmann, K. W. Jucks, A. G. Maki, J.-Y. Mandin, S. T. Massie, J. Orphal, A. Perrin, C. P. Rinsland, M. A. H. Smith, J. Tennyson, R. N. Tolchenov, R. A. Toth, J. Vander Auwera, P. Varanasi, and G. Wagner, 2005: The HITRAN 2004 molecular spectroscopic database. *J. Quant. Spectrosc. Radiat. Transfer*, **96**, 139–204.

Schermaul, R., R. C. M. Learner, D. A. Newnham, R. G. Williams, J. Ballard, N. F. Zobov, D. Belmiloud, and J. Tennyson, 2001a:, The water vapor spectrum in the region 8600–15000 cm^{-1}: Experimental and theoretical studies for a new spectral line database: I. Laboratory measurements. *J. Mol. Spectrosc.*, **208**, 32–42.

Schermaul, R., R. C. M. Learner, D. A. Newnham, J. Ballard, N. F. Zobov, D. Belmiloud, and J. Tennyson, 2001b: The water vapor spectrum in the region 8600–15000 cm^{-1}: Experimental and theoretical studies for a new spectral line database: II. Linelist construction. *J. Mol. Spectrosc.*, **208**, 43–50.

Schmid, B., K. J. Thome, P. Demoulin, R. Peter, C. Matzler, and J. Sekler, 1996: Comparison of modeled and empirical approaches for retrieving columnar water vapor from solar transmittance measurements in the 0.94-mm region. *J. Geophys. Res.*, **101**, 9345–9358.

Schmid, B., J. J. Michalsky, D. W. Slater, J. C. Barnard, R. N. Halthore, J. C. Liljegren, B. N. Holben, T. F. Eck, J. M. Livingston, P. B. Russell, T. Ingold, and I. Slutsker, 2001: Comparison of columnar water-vapor measurements from solar transmittance methods. *Appl. Opt.*, **40**, 1886–1896.

Shiobara, M., J. D. Spinhirne, A. Uchiyama, and S. Asano, 1996: Optical depth measurements of aerosol, cloud, and water vapor using sun photometers during FIRE Cirrus IFO II. *J. Appl. Meteor.*, **35**, 36–46.

Takamura, T, T. Nakajima, and SKYNET community group, 2004: Overview of SKYNET and its Activities. *Proceedings of AERONET workshop*. *El Arenosillo. Opt. Pura y Apl.,* **37**, 3303–3308.

Thome, K., B. M. Herman, and J. A. Reagan, 1992: Determination of precipitable water from solar transmission. *J. Appl. Meteor.*, **31**, 157–165.

Thome, K. J., M. W. Smith, J. M. Palmer, and J. A. Reagan, 1994: Three-channel solar radiometer for the determination of atmospheric columnar water vapor. *Appl. Opt.*, **33**, 5811–5819.

Uchiyama, A., 1992: Line-by-line computation of the atmospheric absorption spectrum using the decomposed Voigt line shape. *J. Quant. Spectrosc. Radiat. Transfer*, **47**, 521–532.